Modeling and design of an observer-based robust controller for a low-cost inverted pendulum based on the H_∞ approach

1st Alejandro Alvarado
TURIX Diagnosis and Control Group
Tecnológico Nacional de México
Tuxtla Gutiérrez, México
AlexAlva9999@gmail.com

2nd Leonardo Gomez-Coronel
TURIX Diagnosis and Control Group
Tecnológico Nacional de México
Tuxtla Gutiérrez, México
M16270670@tuxtla.tecnm.mx

3th Joaquin Dominguez-Zenteno
TURIX Diagnosis and Control Group
Tecnológico Nacional de México
Tuxtla Gutiérrez, México
joaquin.dz@tuxtla.tecnm.mx

4th Vicenç Puig
Institut de Robòtica i Informàtica Industrial, CSIC-UPC
Parc Tecnològic de Barcelona. C Llorens i Artigas 4-6
Barcelona, Spain
vicenc.puig@upc.edu

5th Francisco-Ronay López-Estrada
TURIX Diagnosis and Control Group
Tecnológico Nacional de México
Tuxtla Gutiérrez, México
frlopez@ittg.edu.mx

***Abstract*—The inverted pendulum is a mechanical system with a simple configuration that carries a non-linear, unstable nature widely used in control theory as a benchmark for research. The current research presents the modeling of a low-cost commercially available inverted pendulum and the design of a robust state-feedback controller and a robust observer, following the H_∞ principle and using a low-cost commercially available inverted pendulum system as a reference. Simulated results compare the performance of the designed controller and observer with a conventional LQR controller and observer.**

***Index Terms*—Inverted pendulum; Cart-pole ; Control; Lyapunov; Full-state feedback; Robust controller; Robust observer; H_∞ approach.**

I. Introduction

The inverted pendulum is a widespread case of study for control design due to its simplicity and complex controllability. It is an unstable, non-linear and fourth-order mechanical system that bears several resemblances with other systems, particularly those involving balancing such as loaders, overhead and tower cranes, vehicles like the Segway, and the self-balancing scooter, and even self-balancing and bipedal robotic systems. The control design strategies for the inverted pendulum often focus on three main aspects, the swing-up stage, the vertical stabilization of the pendulum's rod, and the tracking control of the pendulum. This paper is centered exclusively on the second aspect, where the objective is to maintain a vertical position for the rod on its vertical equilibrium point, known as the saddle point, by regulating the cart's movement.

Multiple control strategies are present in the literature to explain, demonstrate and evaluate the performance of different control strategies applied to this particular case of study, serving as a benchmark for researchers. Some studies implement neural networks for various tasks, like in [1] where they use this approach to ease the tracking problem for inverted pendulum systems regarding the repeating tasks of calculating feedforward friction compensations. Similarly, in [2] a neural network is trained to prevent the need to solve the nonlinear dynamics of a bipedal walking system from an inverted pendulum model.

Other approaches involve fuzzy control systems, as in [3] where an event-triggered fuzzy controller with parallel distributed compensation is designed and simulated for an inverted pendulum system to stabilize the generated closed-loop nonlinear systems. In [4] the author develops a multi-level fuzzy controller to stabilize the pendulum with the pendulum bar's flexibility considered in the closed-loop control system and proceeds to simulate the performance of this approach, and in [5] the author designs a fuzzy controller based on Lyapunov stability criteria for a class of twin arm inverted pendulum system, with a black box approach that neglects the need for an accurate mathematical model.

Conventional, model dependent control approaches are also present, as in [6] where the author designs and simulates an LQR controller with a Luenberger observer on a linear inverted pendulum. In [7] a state observer-based linear quadratic Gaussian controller has been designed and simulated, implementing a state feedback controller with a Kalman filter for when unmeasurable states or measurement noise are present. Some articles compare the performance and effectiveness of multiple different control design approaches, as in [9] the author contrasts various types of intelligent and adaptive control techniques, basing the results on computational time, system parameters, and robustness. In [8] the author compares the performance between a conventional PID controller and a fuzzy PID controller in a scenario in which the mathematical model of the system is unknown, all this through the controller's physical implementation on a real linear inverted system. As

mentioned, the inverted pendulum system is a benchmark in control design. Its study allows the analysis and testing of multiple control strategies that can be expanded into larger, more complex systems. This paper aims to design a robust observer-based controller for a low-cost linear inverted pendulum system and contrast its performance with a conventional LQR observer-based controller.

II. Mathematical Modeling

The case of study for these developments consists of a commercial inverted pendulum-cart system, a Wheeltec Mini-Balance, whose layout is shown in Figure 1 and which can be represented by the free body diagram displayed in Figure 2. The physical parameters consist of the mass of the cart M, the mass of the cylindrical rod m, the distance between the center of mass of the rod and the rotation axis l, the moment of inertia of the rod J and both the vertical and horizontal components of the reaction force on the cart-rod junction represented by V and H respectively.

Fig. 1. Linear inverted pendulum.

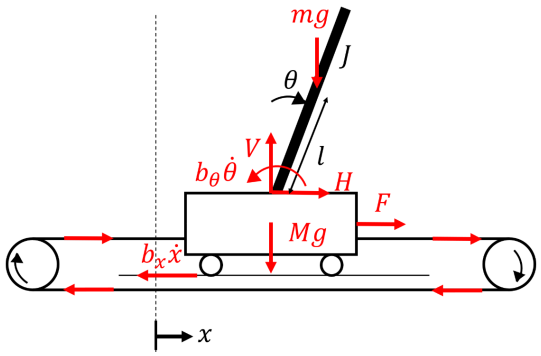

Fig. 2. Model of the linear inverted pendulum.

The system is actuated by the activation of a 12 V DC motor as represented by Figure 3, where there exists a controlled voltage u_a, the internal resistance of R, a counter-electromotive force u_e and a current i_a, all of which yield both a torque T_m and an angular velocity ω_m that is transmitted from the rotor shaft to a pulley-throttled band mechanism, with rotational inertia I, a radius r and a resistive torque of T_d provided by the load. The viscous friction's effect on the cart's linear movement and the rod's angular movement are considered resistive forces of magnitude $b_x\dot{x}$ and $b_\theta\dot{\theta}$ to obtain a more accurate representation of the system.

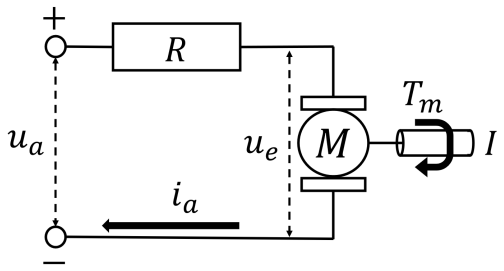

Fig. 3. Model of the DC motor.

The physical constant parameters that were considered for this paper are those provided by the manufacturer, displayed in the Table I.

TABLE I
PHYSICAL CONSTANT PARAMETERS OF THE LINEAR PENDULUM MODEL.

Parameter	Value
m	0.0923 kg
M	0.2275 kg
l	0.1950 m
J	0.0029 kg m^2
R	4.29 Ω
r	0.018 m
K_m	0.183 [Dimensionless]
K_e	0.208 [Dimensionless]
b_x	0 Ns/m
b_θ	0 Ns/m
I	7.083×10^{-6} kg m^2

Analyzing the momentum balance around the center of mass of the rod, the first equation obtained

$$J\ddot{\theta} = Vl\sin\theta - Hl\cos\theta - b_\theta\dot{\theta}, \tag{1}$$

and by applying Newton's Second Law on the cart it is obtained, for the vertical axis

$$V - mg = ma = m\ddot{x} = m\frac{d^2x}{dt^2} = m\frac{d^2\left(l\cos\theta\right)}{dt^2}, \tag{2}$$

and for the horizontal axis,

$$H = m\frac{d^2\left(x + l\sin\theta\right)}{dt^2}. \tag{3}$$

Then, applying Newton's Second Law on the cart yields

$$F - H = M\frac{dx^2}{dt^2} - b_x\dot{x}. \tag{4}$$

From Equations (1), (2), (3) and (4), the nonlinear dynamic model of the pendulum is obtained as (5a) and (5b):

$$(m+M)\,\ddot{x} + ml\ddot{\theta}\cos\theta - ml\dot{\theta}^2\sin\theta + b_x\dot{x} - F = 0, \quad (5a)$$

$$\left(J + ml^2\right)\ddot{\theta} + b_\theta\dot{\theta} + ml\ddot{x}\cos\theta - mgl\sin\theta = 0. \quad (5b)$$

Considering the state variables $[x_1, x_2, x_3, x_4] = [x, \dot{x}, \theta, \dot{\theta}]$, the state-space model is represented by:

$$\begin{bmatrix}\dot{x}_1\\ \dot{x}_2\\ \dot{x}_3\\ \dot{x}_4\end{bmatrix} = \begin{bmatrix} x_2 \\ \frac{\sin(x_3)\,\alpha_1 + F\,J + \cos(x_3)\,\alpha_2 + \alpha_3}{\alpha_4} \\ x_4 \\ -\frac{\cos(x_3)\,\alpha_5 - 2\,\sin(x_3)\,\alpha_6 + \alpha_7}{2\,\alpha_4}\end{bmatrix} \quad (6)$$

where:

$$\begin{aligned}
\alpha_1 =& l^3\,m^2\,{x_4}^2 + J\,l\,m\,{x_4}^2,\\
\alpha_2 =& b_\theta\,l\,m\,x_4 - g\,l^2\,m^2\,\sin(x_3),\\
\alpha_3 =& -J\,b_x\,x_2 + F\,l^2\,m - b_x\,l^2\,m\,x_2,\\
\alpha_4 =& l^2\,m^2\sin(x_3)^2 + M\,l^2\,m + J\,m + J\,M,\\
\alpha_5 =& 2\,F\,l\,m - 2\,b_x\,l\,m\,x_2 + 2\,l^2\,m^2\,{x_4}^2\,\sin(x_3),\\
\alpha_6 =& g\,l\,m^2 + M\,g\,l\,m,\\
\alpha_7 =& 2\,M\,b_\theta\,x_4 + 2\,b_\theta\,m\,x_4.
\end{aligned}$$

The linearization is performed by obtaining the Jacobian matrixes of (6), obtaining the matrixes shown on (7) and (8), where the Jacobian matrix A is defined as:

$$J_A = \begin{bmatrix} 0 & 1 & 0 & 0 \\ 0 & c & d & e \\ 0 & 0 & 0 & 1 \\ 0 & f & g & h \end{bmatrix}, \quad (7)$$

where:

$$\begin{aligned}
c =& -\frac{b_x\left(m\,l^2 + J\right)}{\sigma_3},\\
d =& -\frac{\sin(x_3)\,\beta_2 - \cos(x_3)\,\beta_1 + \beta_5}{\beta_3} - \frac{\beta_{10}}{{\beta_3}^2},\\
e =& \frac{b_\theta\,l\,m\,\cos(x_3) + l\,m\,\sin(x_3)\,\beta_6}{\beta_3},\\
f =& \frac{b_x\,l\,m\,\cos(x_3)}{\left(1 - \cos(x_3)^2\right)l^2\,m^2 + \beta_4 + J\,m + J\,M},\\
g =& \frac{l\,m\,\beta_{11}}{\beta_3} + \frac{\beta_{12}}{{\beta_3}^2},\\
h =& -\frac{x_4\,\sin(2\,x_3)\,l^2\,m^2 + b_\theta\,m + M\,b_\theta}{\beta_3}
\end{aligned}$$

with:

$$\begin{aligned}
\beta_1 =& l^3\,m^2\,{x_4}^2 + J\,l\,m\,{x_4}^2,\\
\beta_2 =& b_\theta\,l\,m\,x_4 - g\,l^2\,m^2\,\sin(x_3),\\
\beta_3 =& l^2\,m^2\sin(x_3)^2 + \sigma_4 + J\,m + J\,M,\\
\beta_4 =& M\,l^2\,m,\\
\beta_5 =& g\,l^2\,m^2\cos(x_3)^2,\\
\beta_6 =& 2\,m\,x_4\,l^2 + 2\,J\,x_4,\\
\beta_7 =& \sin(x_3)\;\beta_1 + \beta_8,\\
\beta_8 =& \cos(x_3)\;\beta_2 + \beta_{17}\\
\beta_9 =& F\,\sin(x_3) + g\,m\,\cos(x_3) + \beta_{13},\\
\beta_{10} =& 2\,l^2\,m^2\,\cos(x_3)\,\sin(x_3)\,\beta_7,\\
\beta_{11} =& -l\,m\left(2\cos(x_3)^2 - 1\right){x_4}^2 + \beta_9,\\
\beta_{12} =& l^2\,m^2\,\cos(x_3)\,\sin(x_3)\,\beta_{15},\\
\beta_{13} =& -b_x\,x_2\,\sin(x_3) + M\,g\,\cos(x_3),\\
\beta_{14} =& l\,m\,\sin(x_3)\,{x_4}^2 + F - b_x\,x_2,\\
\beta_{15} =& \beta_{16} - 2\,g\,l\,m\,\sin(x_3)\,(M+m),\\
\beta_{16} =& 2\,M\,b_\theta\,x_4 + 2\,b_\theta\,m\,x_4 + 2\,l\,m\,\cos(x_3)\,\beta_{14},\\
\beta_{17} =& F\,J - J\,b_x\,x_2 + F\,l^2\,m - b_x\,l^2\,m\,x_2,
\end{aligned}$$

and then, for the B Jacobian matrix:

$$J_B = \begin{bmatrix} 0 \\ \frac{m\,l^2 + J}{l^2\,m^2\sin(x_3)^2 + M\,l^2\,m + J\,m + J\,M} \\ 0 \\ -\frac{l\,m\,\cos(x_3)}{l^2\,m^2\sin(x_3)^2 + M\,l^2\,m + J\,m + J\,M}\end{bmatrix}, \quad (8)$$

The equilibrium point is considered to be when the cart is at the middle of the rail when $x = 0$ and when the rod is at the vertical position when $\theta = 0$. So $x_0 = \begin{bmatrix} x_1^0 & x_2^0 & x_3^0 & x_4^0\end{bmatrix} = \begin{bmatrix} 0 & 0 & 0 & 0\end{bmatrix}$ and $F_0 = 0$. By substitution into (7) and (8) of the constant parameters presented in Table I and the equilibrium point states, the linearized matrices A and B of the dynamic system $\dot{x} = Ax + Bu$, as well as the output vector $y = Cx$ are presented as:

$$A = \begin{bmatrix} 0 & 1 & 0 & 0 \\ 0 & 0 & -1.8395 & 0 \\ 0 & 0 & 0 & 1 \\ 0 & 0 & 32.6837 & 0 \end{bmatrix},\; B = \begin{bmatrix} 0 \\ 3.7139 \\ 0 \\ -10.4286 \end{bmatrix}, \quad (9a)$$

$$C = \begin{bmatrix} 1 & 0 & 0 & 0 \\ 0 & 0 & 1 & 0 \end{bmatrix}, \quad (9b)$$

Since states x_2 and x_4 can not be measured directly, an observer must be designed to implement a controller.

A. Linear controller and observer design for continuous time

Let us consider a dynamic system in the generic form given by:

$$\dot{x} = Ax + Bu, \quad (10)$$

$$y = Cx \quad (11)$$

It is assumed that a number l of sensors provide measurements for the states, so the C matrix is of dimensions $l \times n$. A state-feedback controller with gain K is required to stabilize the system in the vicinity of an equilibrium point by a controlled input of $u = -Kx$, so the controlled system can be written in the generic form of $\dot{x} = (A - BK)\, x$. Using Lyapunov's stability principle, a Lyapunov function $V(x) = x^T P x$ is proposed. When performing the derivative of the Lyapunov function $V(\dot{x}) = x^T P \dot{x} + \dot{x}^T P x$, it can be proven that the linear controller is computed by solving the resulting linear matrix inequality (LMI) (12a) and (12b) where Q is a $n \times n$ symmetric matrix and R a $m \times n$ matrix, where the gains of the controller K are given by $K = RQ^{-1}$.

$$Q > 0, \tag{12a}$$

$$AQ^T - BR + QA^T - R^T B^T < 0. \tag{12b}$$

Due to the fact that x_2 and x_4 are not measured, these should be estimated by mean of Luenberger observer of the form:

$$\dot{\hat{x}} = A\hat{x} + Bu + L(y - \hat{y}), \tag{13}$$

$$\hat{y} = C\hat{x}, \tag{14}$$

where $\hat{x}$ is the estimated state vector, y the estimated output and L the observer gain to be computed. The estimation error is computed as $e = x - \hat{x}$, whose derivative is $\dot{e} = (A - LC)e$; then by considering a Lyapunov function $V(x) = e^T P e$ the gain matrix can be computed fulfilling asymptotic convergence. The observer gain is computed by solving the LMIs:

$$P > 0, \tag{15a}$$

$$PA - WC + A^T P - C^T W^T < 0. \tag{15b}$$

where P is a $\times n$ symmetric matrix and W a $n \times l$ matrix. The gains of the state observer L are given by $= P^{-1}W$.

B. Robust controller and observer design for continuous time

Under disturbances and measurement noise, the system can be expressed as:

$$\dot{x} = Ax + Bu + Rd, \tag{16a}$$

$$y = Cx + Gd, \tag{16b}$$

where R and G are matrices of adequate dimensions, d is the unknown perturbation and noise vector.

To ensure the controller will reduce the effects of perturbations and maintain stability, a robust controller and observer are designed following the H_∞ approach described in [12] and [13], which considers the following performance criteria:

$$\dot{V}(x) + x^T x - \gamma^2 d^T d < 0 \tag{17}$$

for the controller, where $V(x) = x^T P x$, with $P = P^T > 0$ is a quadratic Lyapunov function and γ is the attenuation level to be computed. Then, by considering the above-mentioned criteria the Following LMI is obtained:

$$Q > 0, \tag{18a}$$

$$\begin{bmatrix} AQ - BW - W^T B^T + Q^T A^T & * & * \\ R^T & -\gamma^2 I & * \\ Q^T & 0 & -I \end{bmatrix} < 0, \tag{18b}$$

where Q is a $n \times n$ matrix and W is a $m \times n$ matrix, and R is a $n \times 1$ matrix that defines how every state is affected by a disturbance on the input device. γ is known as a damping factor such that $0 < \gamma < 1$ for the disturbances either in the measuring devices caused by uncertainties of the model. Every $(*)$ corresponds to a corresponding transposed term. The gain $K = WQ^{-1}$ of the robust controller is obtained by solving LMIs (18a) and (18b)

Since the controller K gain given by (18a) and (18b) can reach high values that may not provide a proper control even if the poles of the controlled system fall under the negative semi-plane of the complex axis. A pole placement based on [10] is performed by using LMI (19) instead of (18b) to force the poles of the controlled system inside an LMI region shaped as a circle with radium r_σ and displaced from the imaginary axis a distance d_σ as shown on Figure 4.

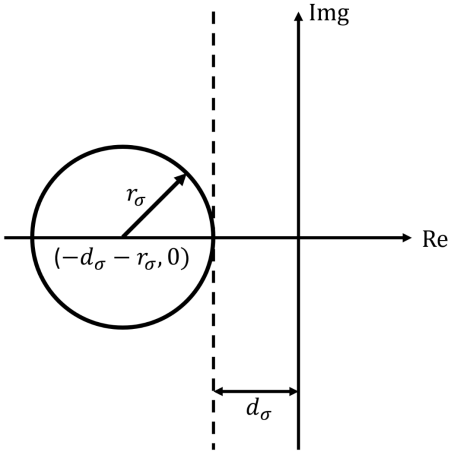

Fig. 4. Circle LMI region.

$$\begin{bmatrix} \mathcal{E} & * & * & * \\ QA^T + W^T B^T + dQ & -r_\sigma Q & * & * \\ R^T & 0 & -I & * \\ CQ + GW & 0 & G & -\gamma^2 I \end{bmatrix} < 0 \tag{19}$$

with $\mathcal{E} = AQ + Q^T A + BW + W^T B^T + 2d_\sigma Q$.

For the observer, the estimation error is defined by $e = x - \hat{x}$. Considering (16) and (13), the dynamic estimation error is $\dot{e} = (A - LC)e + (R - LG)d$. Here the problem is reduced to find a Matrix L such the estimation error converges assyntotically to zero. To achieve this goal the following robust criteria is considered:

$$\dot{V}(e) + e^T e - \gamma^2 d^T d < 0 \tag{20}$$

where $V(e) = e^T P e$, with $P = P^T > 0$ is a quadratic Lyapunov function. The solution of this criteria relies to the following LMI condition:

$$P > 0, \tag{21a}$$

$$\begin{bmatrix} \mathcal{K} & PR - QG + C^T G \\ * & G^T G - \gamma^2 I \end{bmatrix} < 0, \tag{21b}$$

where $\mathcal{K} = PA - QC + A^T P - C^T Q^T + C^T C$. The LMI (21b) can be rewritten through the Schur Complement as:

$$\begin{bmatrix} PA - QC + A^T P - C^T Q^T & * & * \\ R^T P - G^T Q^T & -\gamma^2 I & * \\ C & G & -I \end{bmatrix} < 0. \tag{22}$$

C. Force to voltage conversion

In order to analyze if the resulting magnitudes of the system's force output can be achieved by the commercial pendulum used in this paper, the model of the motor is used to perform the force to voltage conversion, in Equations (23a)-(23c), where K_e is the electromotive force coefficient and K_m is the electromagnetic torque factor.

$$u_a = i_a R + u_e, \tag{23a}$$

$$u_e = K_e \omega_m, \tag{23b}$$

$$T_m = K_m i_a. \tag{23c}$$

On (5a) and (5b) it is possible to express the force F that acts over the cart in terms of the voltage u_a which feeds the DC motor. It is known that the torque T_m given by a DC motor can be modelled as (24):

$$T_m = -\frac{K_m K_e}{R}\omega_m + \frac{K_m}{R}u_a, \tag{24}$$

while the resistance torque provided by the load at the rotor shaft is modeled as (25):

$$T_d = 2Fr. \tag{25}$$

For a DC motor that moves the pulley and the throttled band, the relation between T_m and T_d is given by (26):

$$T_m - T_d = I\frac{d\omega_m}{dt} = I\dot{\omega}_m, \tag{26}$$

where on (26)

$$\dot{x} = \omega_m r \rightarrow \omega_m = \frac{\dot{x}}{r}, \tag{27a}$$

$$\ddot{x} = \dot{\omega}_m r \rightarrow \dot{\omega}_m = \frac{\ddot{x}}{r}, \tag{27b}$$

so by substituting (24), (25), (27a) and (27b) into (26), it can be rewritten as (28)

$$-\frac{K_m K_e}{Rr}\dot{x} + \frac{K_m}{R}u_a - 2Fr = I\frac{\ddot{x}}{r}. \tag{28}$$

So from (28) u_a can be derived as (29)

$$u_a = \frac{2Rr}{K_m}F + \frac{RI}{K_m r}\ddot{x} + \frac{K_e}{r}\dot{x} \tag{29}$$

III. Results

A. Linear controller and observers in continuous time

In the simulations, the R and G matrixes are each a matrix of ones of adequate dimensions. Solving LMIs (12a) and (12b) using Yalmip and SeDuMi on MATLAB the gains of the linear controller K_{Lyapunov} are computed as:

$$K_{\text{Lyapunov}} = \begin{bmatrix} -0.3564 & -0.5897 & -7.000 & -0.8122 \end{bmatrix}. \tag{30}$$

Solving LMI (15a) and (15b), the gains of the linear state observer L_{Lyapunov} are computed as:

$$L_{\text{Lyapunov}} = \begin{bmatrix} 0.8749 & -0.6897 \\ 1.2916 & -2.0693 \\ 0.6897 & 0.8750 \\ 0.2299 & 33.9753 \end{bmatrix}. \tag{31}$$

For comparison, a LQR controller similar to the one designed in [11] was designed, the proposed Q_c and R_c matrixes are shown on (32)

$$Q_c = \begin{bmatrix} 1 & 0 & 0 & 0 \\ 0 & 0 & 0 & 0 \\ 0 & 0 & 1 & 0 \\ 0 & 0 & 0 & 0 \end{bmatrix}, \quad R_c = 100. \tag{32}$$

Gains of the K_{LQR} controller are:

$$K_{\text{LQR}} = \begin{bmatrix} -9.9999 & -6.8802 & -26.3294 & -4.5398 \end{bmatrix}. \tag{33}$$

According to the LMIs (18a)-(18b) and (21a)-(21b), the computed values for the robust controller and observer, K_{H_∞} and L_{H_∞} are:

$$K_{H_\infty} = 1 \times 10^6 \begin{bmatrix} -0.6740 & -0.5908 & -1.9513 & -0.2123 \end{bmatrix}. \tag{34a}$$

$$L_{H_\infty} = \begin{bmatrix} 8.8757 & -1.3966 \\ 8.1681 & -4.5419 \\ 4.4653 & 7.0066 \\ -60.5813 & 70.7792 \end{bmatrix}. \tag{34b}$$

B. Simulation results

For continuous time case, the simulations were conducted using the following gains on the controller and observer:

1) K_{Lyapunov}, L_{Lyapunov}
2) K_{LQR}, L_{Lyapunov}
3) K_{LQR}, L_{H_∞}
4) K_{H_∞}, L_{H_∞}

For every scenario, the initial state of x_3 is 10 deg and the state of x_1 is $0\,\text{m}$, at the middle of the rail. Response in continuous time is presented on Figures 5 and 6. The force F applied to the cart is graphed as shown on Figure 7.

The voltage V demanded by the motor is derived as stated by (29) and its evolution through time is shown on Figure 8.

The LQR controller with the L_{H_∞} observer is the most demanding voltage wise and reaches stability faster than the other controllers.

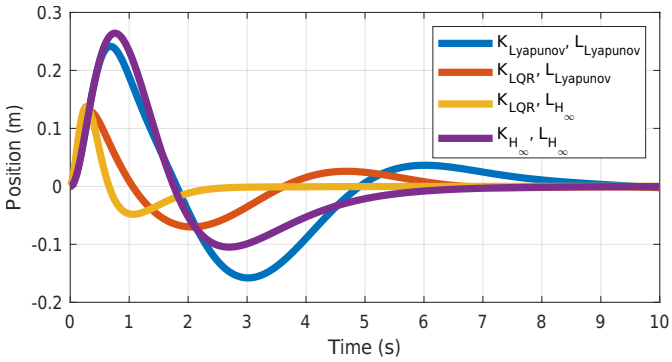

Fig. 5. Displacement of the cart (x_1).

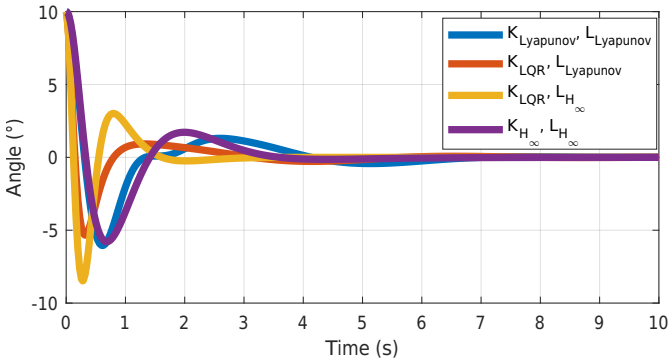

Fig. 6. Angle of the rod in degrees (x_3).

The maximum voltage allowed by the motor is 12 Volts, and the simulation results in figure 8 indicate that all the proposed observer-based controllers can operate within the safe threshold allowed by the motor. However, in the real case, the total length of the rail is $0.44m$, which given the initial condition of the cart being in the center of the rail, results in a maximum allowed displacement of $0.22m$ in any direction, therefore none of the controllers that use a standard full order observer can operate under those conditions, as seen in figure 5.

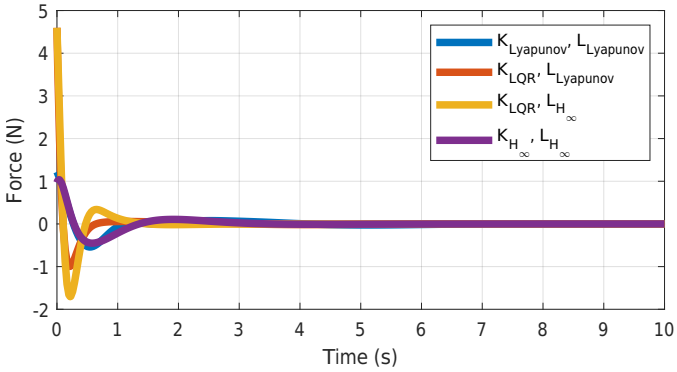

Fig. 7. Force F applied to the cart.

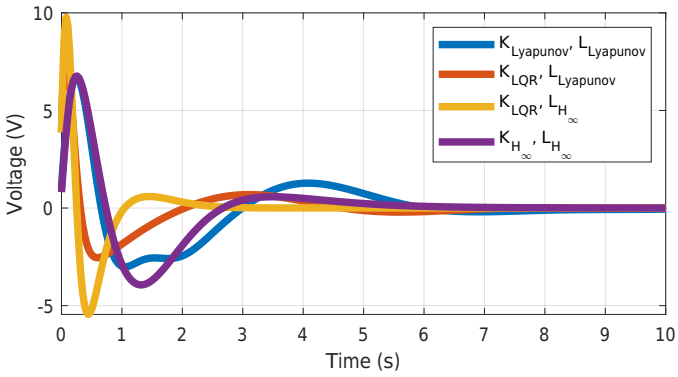

Fig. 8. Voltage u_a demanded by the DC motor VS.

IV. Conclusion

This paper exposed the modelling of the non-linear system of a linear inverted pendulum. A linear observer and controller were designed to stabilize the system when the rod is at a vertical position. Both a controller designed through Lyapunov's stability principle and a LQR controller were implemented and compared in a simulation of the system when the initial state of the angular position of the rod was displaced from stability position. It was observed that the LQR controller provided a faster stabilization of the system, and also it took into account that the input voltage to the DC motor would not be over $12\,\mathrm{V}$, which is the nominal voltage of the system that was used for this analysis. Further work should focus on the implementation of the designed controller into a physical system and compare the results presented in this paper with real measurements provided from experimentation, as well as considering into account the effect of viscous frictions for the linear and angular movements.

References

[1] Ping, Zhaowu, et al. "An improved neural network tracking control strategy for linear motor-driven inverted pendulum on a cart and experimental study." Neural Computing and Applications 34.7 (2022): 5161-5168.

[2] Wang, Ruobing, et al. "Normalized neural network for energy efficient bipedal walking using nonlinear inverted pendulum model." 2019 IEEE International Conference on Robotics and Biomimetics (ROBIO). IEEE, 2019.

[3] Su, Xiaojie, et al. "Event-triggered fuzzy control of nonlinear systems with its application to inverted pendulum systems." Automatica 94 (2018): 236-248.

[4] Pourgholam, Pouriya, and Hamid Moeenfard. "Development of a fuzzy-state feedback regulator for stabilizing a flexible inverted pendulum system." Journal of Vibration and Control (2021): 10775463211042967.

[5] A. Jain, A. Sharma, V. Jately, B. Azzopardi and S. Choudhury, "Real-Time Swing-Up Control of Non-Linear Inverted Pendulum Using Lyapunov Based Optimized Fuzzy Logic Control," in IEEE Access, vol. 9, pp. 50715-50726, 2021, doi: 10.1109/ACCESS.2021.3058645.

[6] Siradjuddin, Indrazno, et al. "State-feedback control with a full-state estimator for a cart-inverted pendulum system." International Journal of Engineering Technology 7.4.44 (2018): 203-209.

[7] Banerjee, Ramashis, and Arnab Pal. "Stabilization of inverted pendulum on cart based on lqg optimal control." 2018 International Conference on Circuits and Systems in Digital Enterprise Technology (ICCSDET). IEEE, 2018.

[8] Rithirun, Chart, Anuchit Charean, and Winyu Sawaengsinkasikit. "Comparison Between PID Control and Fuzzy PID Control on Invert Pendulum System." 2021 9th International Electrical Engineering Congress (iEECON). IEEE, 2021.

[9] A. Krishnan, P. K. U, M. Bukya, P. Randhawa and D. Piromalis, "A Comparative Study on Intelligent and Adaptive Control Techniques on a Nonlinear Inverted Pendulum Cart Mechanism." 2021 9th International Conference on Reliability, Infocom Technologies and Optimization (Trends and Future Directions) (ICRITO), 2021, pp. 1-6.

[10] Mansouri, Badr, et al. "Robust pole placement controller design in LMI region for uncertain and disturbed switched systems." Nonlinear Analysis: Hybrid Systems 2.4 (2008): 1136-1143.

[11] Kumar, E. Vinodh, and Jovitha Jerome. "Robust LQR controller design for stabilizing and trajectory tracking of inverted pendulum." Procedia Engineering 64 (2013): 169-178.

[12] Rigatos, Gerasimos G. "Modelling and control for intelligent industrial systems." adaptive algorithms in robotics and industrial engineering (2011).

[13] Rigatos, G., and P. Siano. "A new nonlinear H-infinity feedback control approach to the problem of autonomous robot navigation." Intelligent Industrial Systems 1.3 (2015): 179-186.